DNA-Guided Assembly of Nanocellulose Meshes

Amrioarei, Alexandru; Barad, Gefry; Czeizler, Eugen; Dobre, Ana-Maria; Icu, Corina; Mitrana, Victor; Pun, Andrei; Pun, Mihaela; Spencer, Frankie; Trandafir, Romic; Tua, Iris

Published in:
Theory and Practice of Natural Computing. TPNC 2018

DOI:
/10.1007/978-3-030-04070-3_20

Publicerad: 01/01/2018

DNA-Guided Assembly of Nanocellulose Meshes

Alexandru Amărioarei[1], Gefry Barad[1], Eugen Czeizler[1,2], Ana-Maria Dobre[1], Corina Iţcuş[1], Victor Mitrana[1], Andrei Păun[1], Mihaela Păun[1], Frankie Spencer[2], Romică Trandafir[1], and Iris Tuşa[1]

[1] National Institute of Research and Development for Biological Sciences, Department of Bioinformatics, Bucharest, Romania
[2] Computational Biomodeling Laboratory, Turku Centre for Computer Science and Department of Computer Science, Åbo Akademi University, Turku, Finland

Abstract. Nanoengineered materials are a product of joint collaboration of theoreticians and experimentalists, of physicists, (bio-)chemists, and recently, of computer scientists. In the field of Nanotechnology and Nanoengineering, DNA (algorithmic) self-assembly has an acknowledged leading position. As a fabric, DNA is a rather inferior material; as a medium for shape, pattern, and dynamic behavior reconstruction, it is one of the most versatile nanomaterials. This is why the prospect of combining the physical properties of known high performance nanomaterials, such as cellulose, graphene, or fibroin, with the assembly functionality of DNA scaffolds is a very promising prospect. In this work we analyze the dynamical and structural properties of a would-be DNA-guided assembly of nanocellulose meshes. The aim is to generate pre-experimental insights on possible ways of manipulating structural properties of such meshes. The mechanistic principles of these systems, implemented through the DNA assembly apparatus, ensure the formation of 2D nanocellulose mesh structures. A key desired feature for such an engineered synthetic material, e.g. with applications in bio-medicine and nano-engineering, would be to control the size of the openings (gaps) within these meshes, a.k.a. its aperture. However, in the case of this composite material, this is not a direct engineered feature. Rather, we assert it could be indirectly achieved through varying several key parameters of the system. We consider here several experimentally tunable parameters, such as the ratio between nanocellulose fibrils and the DNA guiding elements, i.e., aptamer-functionalized DNA origamis, as well as the assumed length of the nanocellulose fibrils. To this aim, we propose a computational model of the mesh-assembly dynamical system, which we subject to numerical parameter scan and analysis.

1 Introduction

As nanotechnology and nanoengineering is evolving, the field of nanoengineered materials becomes more and more in the center of the academic and industrial communities. Current developments in the field include: molecular sieving membranes for highly efficient gas separation [5], hybrid carbon nanostructure for

supercapacitors [24], nanocomposite gels for repair of damaged bones [27], nanotextured surfaces with anti-bacterial properties [11], metalenses - flat surfaces that use nanostructures to focus light [4], exceptionally strong and tough ultrafine fibers [16], nanostructured surface coatings with anti-fouling properties [23], etc. Sometimes, the exceptional properties of these materials are due to material's intrinsic property, e.g. the super-conductance of graphene [24], the high magnetization limit of certain alloys [21], etc. Other times, it is the high resolution arrangements of the material's nanocomponents that give its exceptional characteristics, e.g., the highly aligned calcium silicate hydrate nanoplatelets with bending strength of nacre [17]. To this end, DNA nanotechnology has gain an outstanding recognition for its versatility and addressability at the nanolevel; experimental realizations in the field include highly addressable scaffolds [12], precise pattering [13], 2- and 3D pattern and shape reconstruction [22, 2], and even robotic-like constructs [9, 14].

As a nanomaterial, DNA has also its downsides: it is not particularly rigid, or strong, or tough, it does not conduct electricity, it loses all its interaction properties in dry/dehydrated environments, i.e., outside of buffer solutions, etc. Thus, by pairing the DNA addressability properties with that of a strong nanomaterial and by guiding the precise assembly of the latter we can hope of greatly enhancing its mechanical properties and its applicability. In recent experimental trials we are considering the pairing of DNA nanoconstructs with nanocellulose fibrils in order to create strong and highly aligned nanocellulose meshes for precision filters and membranes. The viability of such a material combination is enhanced by the availability of DNA aptamers for cellulose [3, 26], i.e., 20-50 base long DNA sequences with natural binding affinity for cellulose.

The possibility of using DNA molecules as a structural alignment ligand is presumably one of the first visionary ideas of the DNA nanotechnology community. It is alleged that in its seminal works, Seeman envisioned the use of DNA molecules as a structural confinement medium in order to capture and position proteins within a 3D lattice. The technique would have allowed the formation of synthetic crystals, which could be processed by X-ray crystallography for structural identification. The first successful experimental implementation of such a 3D DNA lattice has been achieved only in 2009 by Seeman and his co-authors [28]. Also the possibility of aligning orthogonally rod-like structures, namely carbon nanotubes, on top of DNA origami structures has been previously demonstrated, see e.g. the results from [10, 6].

The main goal of this study is to generate pre-experimental insights on possible ways of controlling the characteristics of such a DNA-linked nanocellulose mesh, particularly, the average opening window in between the cellulose fibrils of the mesh, a.k.a., the aperture of the mesh. To do this we create two computational models of the assembly dynamical system, which we subject to parameter scan and analysis. One of them will be extensively presented here while the other, due to space limitations, will be just briefly discussed. Our conjecture is that by manipulating a relatively small set of the system's parameters, e.g., the ratio between the input number of cellulose fibrils and the guiding DNA-based

constructs, or the average length of the individual fibrils, we might be able to control the average aperture of the mesh.

From the computational modeling perspective, capturing the complexity of a structural self-assembly system is a notoriously difficult task. This is due to the intrinsic nature of these systems which have a theoretical un-bounded number of different configurations, thus generating a combinatorial explosion of the number of species needed to mathematically capture these systems. In this study we partially overcome this challenge by employing a rule-based modeling methodology, which has a fundamentally different approach of capturing the different "species" of the system [7, 8]. Within this modeling framework molecules are represented as *agents* with a finite number of free *sites*. The sites allow for agent-agent binding, thus generating molecular complexes. *Rules* are defined based on local *patterns* rather than by the full specification of the reactants, and thus provide a compact representation on how agents interact. Thus, rather than handling explicitly a large number of model variables, within this framework we only have a small number of local interaction rules. This makes the rule-based paradigm well suited in handling the problem of the combinatorial explosion of the state space. The applicability of this approach for modeling (protein) self-assembly systems has been previously investigated, see, e.g., [20, 25], including its use for the computational modeling of other types of DNA assembly systems, see, e.g., [15, 1].

2 Materials and Methods

2.1 DNA-Guided Assembly of Nanocellulose Meshes

We want to model in this study the guided assembly of nanocellulose rods (R) with the help of DNA-based macro-structures (O), i.e., DNA origamis [18] (or simply denoted as Origamis), acting as a smart-ligand in between two rods. Moreover, using precise sequence matchings and positioning, one can hope of obtaining a perfect orthogonal positioning of each two intersecting rods, as exemplified in Fig. 1.

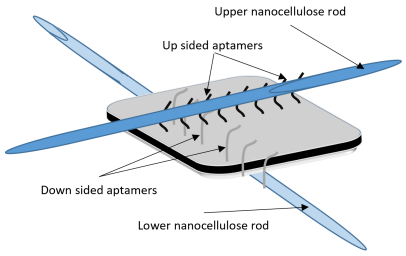

Fig. 1. DNA Origami functionalized by orthogonally aligned cellulose aptamers, placed on opposite sides, and connected to nanocellulose fibrils

While experimental implementations of such systems are currently on incipient stages in our laboratories, in this paper we want to study the possibility

of controlling the size of the autonomously generated average aperture of these meshes, i.e., the average in-between rod gaps, by varying a series of parameters which are achievable from an experimental point of view.

A somewhat simplified discrete dynamical model of the above process can be described as follows: The rods (R) are fixed length objects, with a fixed maximal number l of consecutive docking positions. These docking positions can be occupied only by square 2-dimensional DNA origami (O) constructs. Each O can connect to exactly two Rs, each of them on one of the sides of these structures, such that the two Rs will be placed on orthogonal position, as described in Fig. 1. Thus, once an O is docked on one R's docking position, another R can dock on this O, thus enlarging the assembly; in this study we assume that the R-O binding interactions are irreversible. By subsequent assemblies of R and O elements, the rods will ultimately assemble into a patchy mesh structure, where the holes of this structure will vary depending on the values of several parameters. As in previous study of self-assembly systems, we will assume that only elementary structures, i.e., R and O, can attach to an assembly, and that partial assemblies are not interacting with one another. While we acknowledge that some partial assemblies might interact with one-another, at this moment it is not clear for us if a stability/binding-strength threshold should be added in order to enable such merger, as well as how -or if- such interactions can be captured in our computational model.

Even at this point, we can distinguish between two possible variants for the abstract model of the system. On one hand, we call this model variant M1, we can assume that the minimum gap between two parallel rods is at least the size of an Origami. Indeed, such close parallel rods would be placed on top two Origamis, each on a consecutive docking positions of a third rod, which is perpendicular to both of them, see e.g. Figure 2a). Thus, in our model M1, in between each two parallel Rs there should be at least one minimum space/gap, which is discretized as size 1 (in comparison to the discrete size l of all the rods considered in the system).

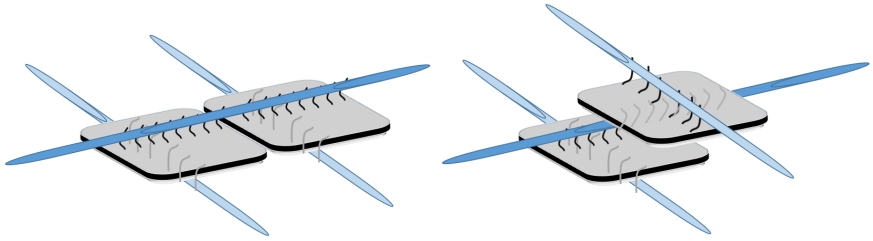

a) b)

Fig. 2. Possible Origami positioning along a nanocellulose fibril. a) Both Origamis are positioned on the same side of the fibril, in which case a minimum (one-Origami wide) inter-fibril gap has to be present. b) The Origamis are positioned on opposite sides of the fibril, in which case in between two parallel fibrils there could be almost no space at all.

On the other hand, we call this model variant M0, it could be that the two Origamis which docked on consecutive positions along the perpendicular rod, have done so, the first on one side of the rod, and the latter on the opposite side, see Figure 2b). Thus, the two Origamis could visually overlap, as they are on slightly different planes. Thus, according to this model variant, the distance in between two parallel rods could be as close to 0 as possible, i.e., will generate a "gap" of size 0 in the discrete universe of this model. Generalizing, we will denote by Mk the model in which the minimum distance between two parallel rods has discrete value k, in relation to the total discrete value l of the length of the rods. In this study we will concentrate over the models M1, M0, and M2.

As previously mentioned, the objective of this study is to analyze whether by manipulating a series of model parameters, which are experimentally achievable, we can influence the average aperture size of the final assembled meshes, i.e., the average size of those spaces which are obtained by interlocking rods, and which are completely surrounded by these rods. The parameters identified by us as experimentally achievable are the ratio between the number of Origamis and rods in the system, and the discrete length l of these rods, respectively. The reasoning for choosing these parameters is as follows. In the classical DNA origami assembly, one important setting for achieving good experimental results was to correctly set the proportion between the concentration of scaffold strand and staple strands. Inspired by this fact, we believe that the ratio between the R and O elements could prove to be an efficient control mechanism for the size of the average mesh aperture. For the second parameter, the discretized length of a rod, i.e., compared to the size of an Origami, we are convinced that this parameter will influence the size of the inter-rod spaces. However, even in this case, we want to estimate the efficiency and strength of this control mechanism.

2.2 Computational Modeling of the Nanocellulose Mesh Dynamical System

We propose first a rule-based modelling methodology for capturing the assembly of the nanocellulose mesh dynamical system. The model is based on the BioNetGen modeling language [7, 8], and implemented using the NFsim [20] and RuleBender [19] computational platforms.

The dynamical system includes two types of agents: rods (R), and Origamis (O), assumed to be introduced in a precise (and experimentally modifiable) concentration ratio $s = O/R$; this ratio s is one of the two parameters which we use in order to adjust/analyze the model dynamics. Each R has a fixed number, l, of consecutive docking positions for O elements, while each O has exactly 2 docking positions for the R elements, placed perpendicularly (and each on a different side of the structure); the parameter l, which is fixed for the entire R population, is the second parameter used to adjust/analyze the model dynamics; while in reality we expect the length of these rods to be variable, for simplification reasons in this study we assume a uniform length for these elements. As in the case of other studies of self-assembly systems, we capture the growth of only one of the assemblies emerging from the system, and, moreover, we assume a

lack of interaction on behalf of partial assemblies, i.e., only elementary R and O units interact with a partial assembly. Also in this case, while we acknowledge that in the experimental setting some partial assemblies might interact with one-another, at this moment it is not clear for us if a stability/binding-strength threshold should be added in order to enable such merger, as well as how -or if- such interactions can be captured in our computational model. Thus, at this point we restrict our model assumptions to the above-mentioned interactions. Thus, the assembly, which starts from a preselected seed of the type R, grows through multiple subsequent associations of O and R elements. Each R embedded in the partial assembly can interact on one of its free docking positions with a free floating O and capture it within the assembly. Similarly, each O embedded in the partial assembly and yet not connected with a second R, interacts with a free floating R on any of its l docking positions (since R is free floating, each of its docking positions is free), and binds this R into the current assembly. In order to keep the O/R ratio constant throughout the process, each time an R (resp. an O) is embedded intro the assembly, a new R (resp. O) element is spawned in the solution. Thus, for each of the l docking sites $d_1, ..., d_l$ we have the following rules in our simulation (we exemplify below for site d_i):

$$\text{R(in}\sim\text{1,}d_i\text{) + O(in}\sim\text{0,x)} \longrightarrow \text{R(in}\sim\text{1,}d_i\text{!1).O(in}\sim\text{1,x!1) + O(x,y,in}\sim\text{0) k1}$$

The above rule is represented in the easily comprehensible BNGL syntax, see, e.g., [7, 8] for a detailed introduction on this modeling formalism and syntax. The sites in and d_i are sites of the agent R, while in, x, and y are sites of O. The symbol $\sim$ denotes the state of one of the sites; in this case, the site in (for both R and O) can be either in state 0, if that agent is free-floating, or in state 1, if it is part of an assembly, i.e. it is linked to another agent. The symbol $!k$, with $k > 0$, denotes the name of a link in between two sites; within a rule, two sites sharing the same link name are connected to one-another. If within a rule a site is not followed by !, it means that site must not be connected to any other site. Finally, the "." symbol in between two agents symbolizes that the two agents are now part of the same complex.

The above rule can be interpreted as follows: if there exists on one hand an agent R within the assembly (in$\sim$1) and with a free (i.e., non-connected) d_i site, and on the other hand a free-floating agent O (in$\sim$0) with a free x site, then the two would bind (non-reversibly) along the $d_i - x$ sites and the R and O agents will became part of the same complex. Also, the site in in of O will change its state from 0 to 1, a new free-floating agent O will be spanned, with free sites x and y (i.e., O(x,y,in$\sim$0)) and the kinetic rate constant of this reaction is k1.

The above rule stands for the addition of a free floating O to the free docking site d_i of an R element from within the assembly. Since the two docking sites, x and y, of the O element are indistinguishable, we can assume without loss of generality that the first docking of O to the assembly is performed on docking site x, while the subsequent docking of an R element is performed on site y.

For the addition a free floating R on its free docking site d_i to the free docking position y of an O element from within the assembly we can write the following BNGL rule:

$$\text{O(in}\sim\text{1,y)} + \text{R(in}\sim\text{0,}d_i\text{)} \longrightarrow \text{O(in}\sim\text{1,y!1).R(in}\sim\text{1,}d_i\text{!1)} + \text{R}(d_1, d_2, \ldots, d_l,\text{in}\sim\text{0) k2}$$

Since both types of reactions described above correspond to the interaction of an R type object with an O type object, we may assume $k1 = k2$; moreover, since there are no actual measurements on the speed of such a reaction, we can assume $k1 = k2 = 1$, by accepting a scaled behavior for the real experimental outcome.

In the initial state of the system we start with 1000 Rs and a constant number of O elements, such that O/R has the given proposed value s. (i.e., if for $s = 0.1$, we set O init. to 100). Also, we introduce exactly one R initial element as within the assembly, i.e., $in \sim 1$, while all its l docking sites are free.

Although BNGL is by default a coarse-grained modeling methodology, and thus will capture the exact structural complexness of the emerging assembly, its output is restricted to pre-defined user queries. For example, we could interrogate the system about the number of R (or O) objects within the assembly at a given time point, or the number of Os which are connected to only one R, etc., but we can not, by default, list the entire emerging assembly structure. On the other hand, NFsim allows the creation of dump files at specific (model) time points, from which we can reconstruct the entire state of the system, including the structure of the emerging assembly, at that time point. Thus, we have created specific Python subroutines for parsing the model dump file at specific time-points, and extract the structural arrangement of the Rods within the current state of the emerging assembly. This structural arrangement is then represented as a 2D integer matrix, the *mesh distribution matrix*, whose entry on point (i, j) has value k, $k \geq 0$, iff there are exactly k superimposed R objects on the (discrete) position (i, j)[3]. In order to trim the output, we crop this matrix according to the mesh surface determined by the area between the coordinates of the top and bottom horizontal R, and the left-most and right-most vertical R.

In a subsequent analysis we use a simplified statistical method for directly generating the above mesh distribution matrix of a final assembled mesh, which we then analyze numerically. Besides the O/R ratio and the l length of the rods, we consider here one more parameter, namely p, the minimal length in-between two possible docking positions. The range of the p variable is from 0, i.e., two consecutive Os can dock on an R on abutting positions, to $l-2$, i.e., the two Os would dock on the opposite heads of an R; in this study we concentrate on the cases when $p = 0$, $p = 1$, and $p = 2$, respectively.

We start with an empty mesh, containing only one R, and we assume there are always 1000 free floating R objects and $1000 \times O/R$ free floating O objects. At each iteration, we select randomly which object, i.e., R or O, to place next, with probability P_R and P_O, respectively, where:

$$P_R = \frac{\#R \times DockR}{\#R \times DockR + \#O \times DockO}, \quad \text{and} \quad P_O = 1 - P_R = \frac{\#O \times DockO}{\#R \times DockR + \#O \times DockO},$$

[3] Note that, by assumption, the R objects intersect one-another at discretized locations, and that all R objects have the same discrete length l

where $\#R$ and $\#O$ are the number of free floating R, respectively O, objects, i.e., 1000 and $1000 \times O/R$, $DockR$ is the number of possible docking positions for the R objects within the current assembly, i.e., the number of O objects within the assembly which are connected only to one R element, and $DockO$ is the maximum number of possible docking positions for the O objects within the current assembly (taking in consideration the minimum gap p allowed in between two consecutive docking positions along the same R object). After a selection is made, the object is placed within the assembly on a position which is randomly chosen from the currently available free positions for that object in the assembly, and the values for $DockO$ and $DockR$ are updated accordingly[4].

3 Results

Our initial analysis of the Cellulose Mesh dynamical system is based on a coarse-grained type modeling performed using the BNGL agent- and rule-based modeling methodology, and is particularly focused on the M1 model described above, i.e., we assume that consecutive O docking positions along a rod are positioned with one gap in between. Using the mesh distribution matrix defined in the previous section, i.e., a matrix representation of the relative positions of inter-connecting R and O objects, we compute the average distribution of inter-rod spaces, a.k.a. the average mesh gaps. Moreover, since the size of these gaps is bound to be influenced by their relative position within the mesh, i.e., central locations are expected to exhibit smaller gap sizes, we can further provide a localized statistic of the average gap size, based on a user-defined zoning granulation of the mesh distribution matrix, and by assigning gaps within these zones according to the position of their center of mass. In this study we have focused over a 4×4 zoning, where the areas are labeled as bellow:

zone 1	zone 2	zone 3	zone 4
zone 5	zone 6	zone 7	zone 8
zone 9	zone 10	zone 11	zone 12
zone 13	zone 14	zone 15	zone 16

In Fig. 3 we provide a series of outputs generated by the model for the case when $|R| = 1000, |O| = 100$, and $l = 10$, i.e., the rods include 10 consecutive docking positions. Namely, we present the time-dependent dynamics of the R and O sub-populations encompassed in the assembly (Fig. 3a) and the zone-specific average gap size (for 7 out of 16 zones), taken at phased time-intervals (Fig. 3b. Note that the system evolves according to a normalized time dynamics, as both the kinetic reaction rates and the sizes of the species populations are themselves normalized.

From the time- and zone-dependent evolution of the average gap size from Fig 3b) we can deduce that in this case, the assembly started forming within zone 11, and latter reached also the remaining zones. While at early stages of

[4] Note that according to our assumption, the $\#R$ and $\#O$ values are constant.

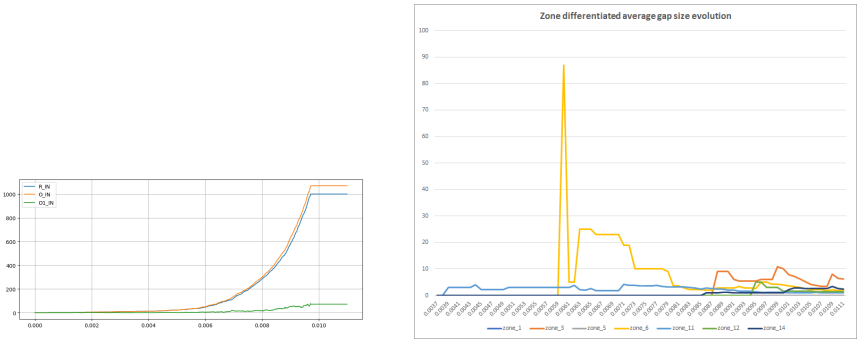

a) b)

Fig. 3. (Normalized) Time-dependent observation for a mesh assembly dynamical system, as captured by the coarse-grained modeling implementation. The parameters of the model are set as $O/R = 0.1, l = 10$, and the dynamics of the system is frozen once the total number of R objects reaches 1000. a) The time dependent dynamics of the R objects within the assembly (R_IN), as well as both all of the O objects in the assembly (O_IN) and those O objects which are connected with only one rod (O1_IN). b) The time dependent evolution of the average gap size for zones 1, 3, 5, 6, 11, 12, and 14, out of all $4 \times 4 = 16$ zones in which we split the assembly surface.

the assembly we had one or several large gaps within zone 6, see the spike in Fig. 3b, later on, by addition of subsequent R objects, these gaps have been split into much smaller enclosures. Another observation from this chart is that as initially predicted, towards later stages of the assembly, the average gap within central zones, as are zone 6, 11, and 12 in our display, are generally lower than those obtained within zones further away from the starting point, namely zones 3 and 14. Meanwhile, for the zones which are further away, i.e., zones 1 and 5, we observed that during the recorded time there has been no gaps generated within these zones, while from the definition of the mesh distribution matrix we know that the rods elongate also over these zones.

The aim of this study is to generate pre-experimental insights on possible ways of controlling and manipulating the average gap size of the DNA-guided assembled nanocellulose meshes. The two parameters which we presume to have the strongest impact on this value and, in the same time, are experimentally achievable, are the ratio s, between the free-floating Origamis and rods placed initially (and thus also throughout the time evolution) in the solution, as well as the (assumed uniform) length l of these rods. During successive in-silico experiments we span s through the values 0.1, 0.5, 1, 5, 10, and l through the values 5, 10, 15, and 20, while keeping the concentration (i.e., particle number) of free-floating R's set to 1000. Also, we simulate each of these scenarios until the number of Rs captured within the mesh reaches 1000.

In each of the above experiments we track the mean aperture of the holes in the mesh, by averaging both over the entire structure, as well as over a 4×4 zoning, thus generating a total of $1+16$ mean values. We repeat each experiment

30 times and we record the median values both per the entire structure, see Fig. 4, and per each of the 16 zones independently.

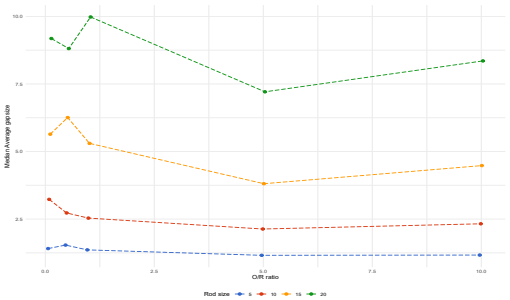

Fig. 4. Results of the coarse-grained model. Dynamics of the assembly-averaged gap size per O/R and rod length variation. Each data point is a median of approx. 30 independent runs. The horizontal axes represent the O/R parameter and the vertical one is the average size of the hole. All assemblies contain 1000 rods.

The data captured in these experiments provides several insights into the outcome of the assembly process. Fist, we can conclude that modifications in the rod's length parameter l generates overall larger differences in the average mesh aperture values than modifications of the O/R parameter does. However, although this latter parameter does influence, at a lower fine-grained resolution, the average gap values exhibits slight value increases at the lower and upper limits of the scanned interval $[0.1, 10]$. Also, as initially anticipated, the average aperture does differ significantly on the positioning it is recorded, with central positions (i.e., zones 6, 7, 9, and 10) closely approaching the minimum value of 1, side positions (zones 2, 3, 5, 8, 9, 12, 14, and 15) diverging from this minimum, and corner positions (zones 1, 4, 13, and 16) generating almost no gap at all. Moreover, these diverging recordings from the absolute minimum hole size of 1 recorded in the central positions seem to be increasing with O/R parameter spanning towards the lower and upper bounds of the considered interval. Overall, we consider these results encouraging, as they provide a clear indication of the possibility of controlling the results of the assembly process, and of being able to engineer nanocellulose meshes with custom-build average apertures.

Despite the previous being a coarse-grained modeling approach, some of the structural properties of the assembled structure cannot be captured in the above modeling framework, and this could be a source of errors in modeling the systems dynamics and its structural characteristics. Indeed, the BNGL modeling approach, which is based on local interactions, captures very well the "docking" process of free-floating R and O objects within the assembly. However, it does not record the intersections these objects generate with other objects in the assembly (i.e., other than their initial docking partners); indeed, all these intersections and the gaps they form, are subsequently analyzed based on the dump files generated at desired (model-) time points within the simulation. In particular, this implies that these undetected rod overlaps would generate an increase number of O (and subsequently R) overlapped docking positions, which in reality would not be reachable, as they would become encapsulated in the surrounding over-

lapped objects. Thus, we have considered a special tailored stochastic modeling approach described succinctly in Section 2.2 which keeps track of the overlying mesh structure during its dynamical evolution. Due to the lack of space here, the stochastic model will be presented in a latter development of this work.

4 Discussion

Computational modeling of structural self-assembly system is known to be challenging, and our attempts to capture the dynamics of the cellulose-assembly system confirmed this situation. We have considered two modeling methodologies, one of them discussed in detail and the other just informally presented, both with specific advantages and weaknesses. The coarse-grained methodology, implemented in NFsim, is indeed constructed as a model for a bio-chemical process: it encompasses a time-dynamics, it is governed by the Mass Action kinetics laws, and its simulation is running in acceptable time, even for larger models, e.g. when the fibril length is 40. On the other hand, this model is not able to fully capture the structural complexity of the system. One of its strongest shortcomings is that this current model cannot keep track of subsequent R object overlapping and, moreover, it is not able to disable the O docking sites on these overlapped sites. Thus, new R attachments have an abnormally high probability to attach to already agglomerated (and multiple overlapped) areas. As a consequence, lateral growth of the assembly is inhibited to some extent.

Within the intended tailored stochastic model, we hope to have more control over the underlying structure, and thus we can de-activate the unreachable docking positions. It seems that the assemblies obtained in the tailored stochastic model are larger, and with less overlaps.

However, in this setting, we lose any notion of time-dynamics, as the model does not take time into consideration. Also, for this computational model, simulation time becomes quickly prohibitive.

Acknowledgment. This work was supported by the Academy of Finland through grant 311371/2017 and by the Romanian National Authority for Scientific Research and Innovation, through the POC grant P_37_257.

References

1. A. Amărioarei et al., One dimensional DNA tiles self assembly model simulation, *Int. Journ. of Unconventional Computing*, accepted 2018.
2. E. Benson et al., DNA rendering of polyhedral meshes at the nanoscale, *Nature*, 523(7561): 441–444, 2015.
3. J. B. Boese and R. R. Breaker, In vitro selection and characterization of cellulose-binding DNA aptamers, *Nucleic Acids Res.*, 35(19):6378-6388, Oct. 2007.
4. W. T. Chen et al., A broadband achromatic metalens for focusing and imaging in the visible, *Nature Nanotechnology*, 13: 220-226, 2018.
5. L Ding et al., MXene molecular sieving membranes for highly efficient gas separation, *Nature Communications*, 9(155), 2018.

6. A. P. Eskelinen et al., Assembly of single-walled carbon nanotubes on DNA-origami templates through streptavidin–biotin interaction, *Small*, 7(6):746–750, 2011.
7. J. R. Faeder et al., Rule-based modeling of biochemical networks, *Complexity*, 10:22-41, 2005.
8. J. R. Faeder, M. Blinov, and W. Hlavacek, Rule-based modeling of biochemical systems with BioNetGen. In: *Systems Biology* vol. 500, Humana Press, 2009, pp. 113–167.
9. H. Gu et al., A proximity-based programmable DNA nanoscale assembly line, *Nature*, 465:202-205, May 2010.
10. T. M. Hareem et al., Self-assembly of carbon nanotubes into two-dimensional geometries using DNA origami templates, *Nature Nanotechnology*, 5:61-66, 2010.
11. Y. Jang et al., Inhibition of bacterial adhesion on nanotextured stainless steel 316L by electrochemical etching, *ACS Biomaterials Science & Engineering*, 4(1):90-97, 2018.
12. A. Kuzyk, K. T. Laitinen and P. Törmä, DNA origami as a nanoscale template for protein assembly, *Nanotechnology*, 20(23):235305, May 2009.
13. A. Kuzyk et al., DNA-based self-assembly of chiral plasmonic nanostructures with tailored optical response, *Nature*, 483:311-314, March 2012.
14. K. Lund et al., Molecular robots guided by prescriptive landscapes, *Nature*, 465:206-210, May 2010.
15. A. Mohammed, E. Czeizler and E. Czeizler, Computational modelling of the kinetic Tile Assembly Model using a rule-based approach, *Theoretical Computer Science*, 701:203 - 215, 2017.
16. J. H. Park and C. G. Rutledge, Ultrafine high performance polyethylene fibers, *Journal of Materials Science*, 53(4):3049–3063, Feb. 2018.
17. A. Picker et al., Mesocrystalline calcium silicate hydrate: A bioinspired route toward elastic concrete materials, *Science Advances* 3(11), 2017.
18. P. W. K. Rothemund, Folding DNA to create nanoscale shapes and patterns, *Nature*, 440:297–302, March 2006.
19. A.M. Smith et al., RuleBender: Integrated modeling, simulation and visualization for rule-based intracellular biochemistry, *BMC Journal of Bioinformatics*, 13:1-16, June 2012.
20. M. Sneddon, J. Faeder, and T. Emonet, Efficient modeling, simulation and coarse-graining of biological complexity with NFsim, *Nature Methods*, 8(2):177–183, 2011.
21. R. J. Snow et al., Large moments in bcc FexCoyMnz ternary alloy thin films, *Applied Physics Letters*, 112(7):072403, 2018.
22. G. Tikhomirov, P. Petersen, and L. Qian, Fractal assembly of micrometre-scale DNA origami arrays with arbitrary patterns, *Nature*, 552:67-71, Dec. 2017.
23. C. S. Ware et al., Marine antifouling behavior of lubricant-infused nanowrinkled polymeric surfaces, *ACS Applied Materials & Interfaces*, 10(4):4173-4182, 2018.
24. G. Xiong et al., Bioinspired leaves-on-branchlet hybrid carbon nanostructure for supercapacitors, *Nature Communications*, 9(790), 2018.
25. J. Yang and W. S. Hlavacek, The efficiency of reactant site sampling in network-free simulation of rule-based models for biochemical systems, *Physical Biology*, 8(5):055009, Oct. 2011.
26. Q. Yang et al., DNA ligands that bind tightly and selectively to cellobiose, *Proceedings of the National Academy of Sciences* 95(10):5462–5467, 1998.
27. K. Zhang et al., Nanocomposite hydrogels stabilized by self-assembled multivalent bisphosphonate-magnesium nanoparticles mediate sustained release of magnesium ion and promote in-situ bone regeneration, *Acta Biomaterialia*, 64:389-400, 2017.
28. J. Zheng et al., From molecular to macroscopic via the rational design of a self-assembled 3D DNA crystal, *Nature*, 461(7260):74-77, Sept. 2009.